

## Controlling the Dynamic Behavior of Heterogeneous Self-Oscillating Gels

Victor V. Yashin<sup>a)</sup>, Seiichi Suzuki<sup>b)</sup>, Ryo Yoshida<sup>b)</sup> and Anna C. Balazs<sup>a)\*</sup>

<sup>a)</sup> Chemical Engineering Department, University of Pittsburgh, Pittsburgh, PA 15261, USA.

<sup>b)</sup> Department of Materials Engineering, Graduate School of Engineering, The University of Tokyo, Tokyo, 113-8656, Japan.

\*<sup>a)</sup> Corresponding author, e-mail: [balazs@pitt.edu](mailto:balazs@pitt.edu)

### ELECTRONIC SUPPLEMENTARY INFORMATION (ESI)

Notations:

- (#) Numbered equation in the main text
- (S#) Numbered equation in ESI
- [#] Reference in ESI

#### A. Gel Lattice Spring Model

We consider a layer of swollen polymer gel located in the  $XY$  plane. The layer thickness is given by the fixed value of  $\lambda_{\perp}H_0$ , where  $H_0$  is the thickness of the undeformed gel, and  $\lambda_{\perp}$  is the degree of swelling in the transverse direction. In the undeformed state, the gel geometry is captured by triangulation in the  $XY$  plane. Each undeformed element is characterized by the same values of the volume fraction of polymer  $\phi_0$  and the cross-link density  $c_0$ . The undeformed elements belonging to the BZ patches are also characterized by the concentration of the ruthenium catalyst  $c_{Ru}$ , which is assumed to be constant within a patch but can vary from patch to patch.

The nodes of the triangular mesh are labeled (global labeling) by the integer number  $N$ ,  $1 \leq N \leq N_{tot}$ , where  $N_{tot}$  is the total number of nodes, and  $\mathbf{X}_N$  is the spatial position of node  $N$  in the undeformed state. Upon deformation,  $\mathbf{X} \rightarrow \mathbf{x}(\mathbf{X}, t)$ ; that is, a point with the initial (undeformed) coordinates  $\mathbf{X}$  moves to a new position  $\mathbf{x}(\mathbf{X}, t)$  during the period of time  $t$ . The mesh nodes move together with the gel (i.e., they are “frozen” into the gel), so that  $\mathbf{X}_N \rightarrow \mathbf{x}_N(t)$ , where  $\mathbf{x}_N$  is the actual position of node  $N$  at the moment of time  $t$ . In addition to the spatial position, each node is characterized by the time-dependent local values of the concentrations of the BZ reagents  $u$  and  $v$ , and the time-dependent volume fraction of polymer

$\phi$ . To derive the equations of motion for the nodal coordinates and concentrations, we use a finite element approximation, as described below. The time-dependent nodal values of  $\phi$  are determined through  $\phi_0$  and the nodal coordinates (see below).

In a mesh, each node is the vertex of a cell, which consists of the triangular elements adjoining the node. A cell is labeled by the same integer number as its vertex node, i.e., node  $N$  is the vertex of cell  $N$ . We describe each cell by the piecewise linear function  $\Phi_N(\mathbf{x})$ , which equals 1 at  $\mathbf{x}_N$  and zero at the neighboring nodes (see Fig. S1a). In the context of finite element methods, the function  $\Phi_N(\mathbf{x})$  is known as the global shape function [1] or the hat-function. The hat-function satisfies a number of properties, such as

$$\Phi_N(\mathbf{x}_M) = \delta_{NM}, \quad \sum_N \Phi_N(\mathbf{x}) = 1, \quad \sum_N \mathbf{x}_N \Phi_N(\mathbf{x}) = \mathbf{x}. \quad (\text{S1})$$

The above properties make the hat-function useful for a linear interpolation of the data. Namely, if some variable,  $g$ , is defined at the nodal points,  $g_N$ , then the linear interpolation of the data over the entire region is provided by

$$\tilde{g}(\mathbf{x}) = \sum_N g_N \Phi_N(\mathbf{x}) \quad (\text{S2})$$

The tilde symbol denotes that  $\tilde{g}$  is an approximation to  $g$ .

It has been demonstrated that the hat-function can also be used for coarse-graining, i.e., by formulating an approximate, contracted description of a system via a drastic reduction of the degrees of freedom that are taken into account [2,3]. For example, a value  $\rho(\Gamma)$ , which depends on the coordinates of many particles  $\Gamma$ , can be coarse-grained through the introduction of the density  $\rho_N$ , which is localized to node  $N$  by integration with the hat-function  $\Phi_N$ . Namely,  $\rho_N = V_N^{-1} \int \rho \Phi_N d\Gamma$ , where  $V_N$  is the weight factor of cell  $N$  defined as

$$V_N = \int \Phi_N d\mathbf{x} \quad (\text{S3})$$

As a result, the system is described in terms of a relatively small number of variables  $\rho_N$  defined at the mesh nodes [2,3].

In this paper, we adopt the above procedure to perform the spatial discretization of the partial differential equations that describe the heterogeneous BZ gels. The nodal values are defined as

$$g_N = V_N^{-1} \int g(\mathbf{x}) \Phi_N(\mathbf{x}) d\mathbf{x} \quad (\text{S4})$$

where  $g(\mathbf{x})$  denotes some model variable, e.g., the velocity of the polymer and the concentrations of the BZ reactants. Then, the evolution of  $g_N$  in time is determined by applying the model equations, e.g., eqs. (1)–(3), to eq. (S4). Finally, the linear interpolation given in eq. (S2) is used to find the approximate solution  $\tilde{g}(\mathbf{x})$  in the entire domain. In what follows, we omit the tilde symbol, which denotes approximation, if it does not lead to an ambiguity.

We take into account that the hat-function  $\Phi_N$  depends on both  $\mathbf{x}$  and  $t$  as the triangular mesh moves together with the BZ gel. In order to be a piecewise linear function of  $\mathbf{x}$  at any moment of time  $t$ , the function  $\Phi_N$  must obey the following equation:

$$\partial_t \Phi_N + (\mathbf{v}_p \cdot \nabla) \Phi_N = 0 \quad (\text{S5})$$

where  $\mathbf{v}_p$  is the velocity of the polymer. The above kinematic equation is equivalent to the assumption that within any triangular element, the deformation of gel  $\mathbf{X} \rightarrow \mathbf{x}(\mathbf{X}, t)$  is described by linear functions of the nodal coordinates. In the latter case, the point  $\mathbf{X}$  in the undeformed element and the point  $\mathbf{x}(\mathbf{X})$  in the deformed element are characterized by the same local triangular coordinates [1], so that  $\Phi_N(\mathbf{x}, t) = \Phi_N(\mathbf{X}, 0)$  and  $d\Phi_N/dt = 0$ . It is worth noting that eq. (S5) allows us to use eq. (S2) for the interpolation of the velocity of the polymer  $\mathbf{v}_p = d\mathbf{x}(\mathbf{X}, t)/dt$ , i.e.,

$$\mathbf{v}_p(\mathbf{x}, t) = \sum_N \mathbf{v}_N(t) \Phi_N(\mathbf{x}, t) \quad (\text{S6})$$

where  $\mathbf{v}_N$  is the velocity of node  $N$ . Below, the time dependence of  $\mathbf{v}_N$  and all other nodal values is assumed, but not shown explicitly for simplicity.

Differentiation of eq. (S4) with respect to the time  $t$  yields the following equation for the nodal value  $g_N$

$$dg_N/dt = -g_N V_N^{-1} dV_N/dt + V_N^{-1} \int \Phi_N [\partial_t g + \nabla \cdot (g \mathbf{v}_p)] d\mathbf{x} . \quad (\text{S7})$$

To obtain the above equation, we utilized eq. (S5) and took into account that by definition,  $\Phi_N(\mathbf{x}) \geq 0$  inside cell  $N$ , and  $\Phi_N(\mathbf{x}) = 0$  at the cell boundary and outside it. Equation (S7) is used for the discretization of the reaction diffusion equations: eqs (1)-(3), (8) and (9).

We begin by formulating the discretized reaction-diffusion equations for the BZ gel, eqs. (1)-(3). First, we apply eq. (S7) to determine the time evolution of the nodal value of the volume fraction of polymer  $\phi_N$ . Substitution of eq. (3) into the right-hand side (r.h.s.) of eq. (S7) gives

$$d(\phi_N V_N) / dt = 0 \quad (\text{S8})$$

It can be shown (see Section B below) that the weight factor  $V_N$ , which is defined by eq. (S3), is linearly proportional to the area of the cell,  $A_N$ ; namely,  $V_N = A_N / 3$ . Therefore, eq. (S8) means simply that the amount of polymer within each cell does not change in time. Hence, eq. (S8) can be re-written as

$$\phi_N = \frac{\phi_0 A_N^{(0)}}{\lambda_{\perp} A_N} \quad (\text{S9})$$

where  $A_N^{(0)}$  is the area of cell  $N$  in the undeformed state. Note that eq. (S9) defines  $\phi_N$  as an algebraic function of the coordinates of the cell nodes in the undeformed and current states.

Next, by substituting eq. (2) into the r.h.s. of eq. (S7), we obtain the following equation for the time-dependent nodal value of the oxidized catalyst  $v_N$ :

$$dv_N / dt = -v_N V_N^{-1} dV_N / dt + V_N^{-1} \int \Phi_N \varepsilon G d\mathbf{x} . \quad (\text{S10})$$

It is convenient to introduce the partial value  $\mathbf{v}_N = v_N / \phi_N$ , which is the mole fraction of the oxidized catalyst in the polymer network. In effect, the spatial distribution of the oxidized catalyst is sought to be in the form  $v(\mathbf{x}) = \sum_N \mathbf{v}_N \phi_N \Phi_N(\mathbf{x})$ , where  $\phi_N$  is given by eq. (S9). The nodal value  $\mathbf{v}_N$  obeys the following equation, which was obtained by using eqs. (S8) and (S9):

$$d\mathbf{v}_N / dt = \frac{3\lambda_{\perp}}{\phi_0 A_N^{(0)}} \int \Phi_N \varepsilon G d\mathbf{x} . \quad (\text{S11})$$

It is worth noting that the nodal value  $\mathbf{v}_N$  varies in time due to the BZ reaction only. The reaction rate is represented as a function of the nodal values of the BZ reagents. For the latter purpose, the concentration fields within the triangular elements, which form the cell, are calculated using the linear interpolation between the corresponding nodal values, and then the integration is performed on the r.h.s. of eq. (S11) (see Section B below).

The equation for the nodal value  $u_N$ , the concentration of the activator, is obtained by applying eq. (S7) to eq. (1). The equation for  $u_N$  is further simplified by reformulating it in terms of the partial value  $\mathbf{u}_N = (1 - \phi_N)^{-1} u_N$ , which is the concentration of the activator in solution, and hence,  $u(\mathbf{x}) = \sum_N \mathbf{u}_N (1 - \phi_N) \Phi_N(\mathbf{x})$ . The equation for  $\mathbf{u}_N$  can be written as

$$(1 - \phi_N) d\mathbf{u}_N / dt = -\mathbf{u}_N V_N^{-1} dV_N / dt + V_N^{-1} \int (\mathbf{J}_u \cdot \nabla \Phi_N) d\mathbf{x} + V_N^{-1} \int \Phi_N F d\mathbf{x} . \quad (\text{S12})$$

Here,  $\mathbf{J}_u$  is the flux of the activator

$$\mathbf{J}_u = -\mathbf{u} \mathbf{v}_p - (1 - \phi) \nabla \mathbf{u} , \quad (\text{S13})$$

where  $\mathbf{u} = (1 - \phi)^{-1} u$ . The factor  $V_N^{-1} dV_N / dt$  in the first term on the r.h.s of eq. (S12) is an algebraic function of the nodal coordinates  $\mathbf{x}_N$  and velocities  $\mathbf{v}_N$  that can be determined through a purely geometrical consideration. To perform the integration in the second term on the r.h.s. of eq. (S12), the linear interpolation is used to represent the velocity of the polymer  $\mathbf{v}_p$  and the concentration  $\mathbf{u}$  as linear functions of the respective nodal values (see Section B below). Specifically, eq. (S6) is utilized to calculate  $\mathbf{v}_p(\mathbf{x})$ , and the concentration of the activator in solution is calculated as  $u(\mathbf{x}) = \sum_N \mathbf{u}_N \Phi_N(\mathbf{x})$ . Finally, the reaction rate contribution, which is given by the third term on the r.h.s. of eq (S12), is determined through the same approach as described above for eq. (S11).

Equations (S11) and (S12) describe the BZ reaction in a catalyst-containing region of the gel. The latter equations must be accompanied by the description of the gel dynamics. The dynamical behavior of the gel is captured by the equations of motion for the nodal points

$$d\mathbf{x}_N / dt = \mathbf{v}_N , \quad (\text{S14})$$

where the nodal velocity is determined according to eqs. (10) and (S4), i.e.,

$$\mathbf{v}_N = V_N^{-1} \int \Phi_N \phi_0 \phi^{-1} M(\phi) (\nabla \cdot \hat{\mathbf{c}}) d\mathbf{x} \quad (\text{S15})$$

In the above equation,  $M$  is the gel mobility defined as

$$M(\phi) = \Lambda_0 (1 - \phi) (\phi_0 / \phi)^{1/2} \quad (\text{S16})$$

The integration on the r.h.s. of eq. (S15) is carried out separately over the elements forming the cell. The elements of cell  $N$  are labeled by the integer number  $e_N$ ,  $1 \leq e_N \leq E_N$ ,

where  $E_N \geq 1$  is the total number of elements adjoining node  $N$  (see Fig. S1b). Within each element, the nodes are labeled by  $n=1,2,3$  (local labeling) in the counter clockwise direction (see Fig. S1c) starting from the cell vertex. For element  $e_N$ , we also introduce the edge vectors  $\mathbf{d}_n(e_N)$ ,  $n=1,2,3$ , as shown in Fig. S2, so that the edge  $n$  is located opposite to the node  $n$ , and  $\sum_n \mathbf{d}_n(e_N) = 0$ . The area of element  $e_N$  is denoted as  $A(e_N)$ , and the cell area is  $A_N = \sum_{e_N} A(e_N)$ . The volume fraction of polymer is spatially uniform within each element, and determined by an equation similar to eq. (S9), i.e.,  $\phi = \phi_0 A_0 (\lambda_{\perp} A)^{-1}$ , where  $A_0$  is the element area in the undeformed state, and the element label is omitted for brevity. It can be shown (see Section B below) that after the integration, the r.h.s. of eq. (S15) can be expressed as a sum of the elemental contributions, namely,

$$\mathbf{v}_N = A_N^{-1} \sum_{e_N} A(e_N) \mathbf{M}(e_N) \mathbf{F}(e_N) . \quad (\text{S17})$$

where  $\mathbf{M}(e_N)$  is the mobility, eq. (S16), calculated at  $\phi = \phi(e_N)$ , and  $\mathbf{F}(e_N)$  is the force acting on the node  $N$  from within the element  $e_N$ . We note that the bold faced symbol  $\mathbf{F}$ , which denotes the force (i.e., a vector), should not be mistaken with the italicized symbol  $F$  denoting the BZ rate function (i.e., a scalar) in eq. (4). The elemental force  $\mathbf{F}$  is determined by the following equation (the element label  $e_N$  is omitted):

$$\mathbf{F} = \frac{3c_0}{2A_0} [-\cot(\alpha_0) \mathbf{d}_2 + \cot(\beta_0) \mathbf{d}_3] + \frac{3\lambda_{\perp}}{2A_0} (\mathbf{e}_3 \times \mathbf{d}_1) P . \quad (\text{S18})$$

The first term on the r.h.s. of the above equation describes the linear spring-like forces between the neighboring nodes. Besides the crosslink density  $c_0$ , the spring constants depend on the size and shape of the undeformed triangular element that enter eq. (S18) through the element area  $A_0$  and the alternate angles  $\alpha_0$  and  $\beta_0$  (see Fig. S2), respectively. The second contribution to the elemental force  $\mathbf{F}(e_N)$ , eq. (S18), is due to the isotropic pressure  $P(e_N)$ , which is the isotropic part of eq. (10),  $P = \pi_{FH}(\phi) + \chi^* v \phi + c_0 \phi (2\phi_0)^{-1}$ , calculated at  $\phi = \phi(e_N)$  and  $v = v(e_N)$ . The value of  $v(e_N)$  is defined as the average concentration of the oxidized catalyst in the element  $e_N$ .

Thus, eqs. (S11), (S12), (S14), (S17) and (S18) taken together describe the chemo-mechanical behavior of the BZ gel represented by the triangular elements of arbitrary size and shape (unstructured triangular mesh). We note that the formulation presented here is a generalization of the gLSM approach developed previously for the case of equal quadratic elements [4], and allows us to model BZ gels of a complex geometry.

The gLSM approach developed for the BZ gel can be extended immediately to the case of a heterogeneous gel, which consists of both the reactive and nonreactive regions [5]. The reaction and diffusion of the activator  $u$  in the nonreactive gel is described by eq. (S12), in which the BZ reaction rate function  $F$  is taken in the form  $F(u) = -u^2$ . The nodal velocity is determined according to eqs. (S17) and (S18), in which the isotropic pressure is calculated at  $v = 0$ .

A special treatment is needed to describe the reaction and diffusion of the activator  $u$  in the outside solution. In general, the shape of the heterogeneous gel varies in time, so eq. (9) must be solved under the constraint of moving boundary conditions. To solve the latter problem, we extend the triangular mesh over the entire system, including the outside solution, and fix the nodal positions at the outer boundary of the system. Then, we assume that the mesh external to the gel behaves like a fictitious elastic body, which deforms when the gel boundary moves, but does not impose a force back onto the gel boundary. As a result, eq. (9) can be solved using an approach similar to that described above.

Specifically, we describe the mesh outside the gel as a compressible neo-Hookean solid, characterized by the following stress-strain equation [6]:

$$\hat{\boldsymbol{\sigma}}^* = c^* J^{-1} (\hat{\mathbf{B}} - \hat{\mathbf{I}}) + K^* J^{-1} \log(J) \hat{\mathbf{I}} \quad (\text{S19})$$

Here,  $J$  is the local volumetric change, and  $c^*$  and  $K^*$  are the model parameters, which are proportional to the shear and bulk moduli, respectively [6,7]. The dynamics of this fictitious solid is described by the relaxational equation  $\mathbf{v}^* = M^* \nabla \cdot \hat{\boldsymbol{\sigma}}^*$ , where  $\mathbf{v}^*$  and  $M^*$  are the velocity and mobility, respectively. The same procedure as outlined above, cf. eqs. (S14) and (S17), yields the following equations for the moving nodal points:

$$d\mathbf{x}_N^* / dt = \mathbf{v}_N^* , \quad (\text{S20})$$

$$\mathbf{v}_N^* = M^* A_N^{-1} \sum_{e_N} \mathbf{F}^*(e_N) . \quad (\text{S21})$$

Here, the elemental force is [cf. eq. (S18)]

$$\mathbf{F}^* = \frac{3}{2} c^* [-\cot(\alpha_0) \mathbf{d}_2 + \cot(\beta_0) \mathbf{d}_3] + \frac{3}{2} A_0 A^{-1} (\mathbf{e}_3 \times \mathbf{d}_1) [c^* - K^* \log(AA_0^{-1})] , \quad (\text{S22})$$

and all of the notation is the same as in eqs. (S17) and (S18). The approximate solution of eq. (9) is provided by the linear interpolation between the nodal values,  $u(\mathbf{x}) = \sum_N u_N \Phi_N(\mathbf{x})$ , and the following equation should be solved to obtain the nodal values  $u_N$  [cf. eq. (S12)]:

$$du_N / dt = -u_N V_N^{-1} dV_N / dt + V_N^{-1} \int (\mathbf{J}_u \cdot \nabla \Phi_N) d\mathbf{x} + V_N^{-1} \int \Phi_N u^2 d\mathbf{x} . \quad (\text{S23})$$

In eq. (S23), the flux of the activator  $\mathbf{J}_u$  is defined as [cf. eq. (S13)]

$$\mathbf{J}_u = -u \mathbf{v}^* - \nabla u , \quad (\text{S24})$$

where  $\mathbf{v}^* = \sum_N \mathbf{v}_N^* \Phi_N(\mathbf{x})$ , and the nodal velocity  $\mathbf{v}_N^*$  is calculated according to eq. (S21).

Finally, we note that the continuity of the activator concentration  $u$  and its flux at the gel-solution boundary is automatically fulfilled in the approach developed here. This is because the reaction and diffusion of the activator within the swollen gel are described in terms of the variable  $\mathbf{u} = u(1 - \phi)^{-1}$ , which is the concentration of the activator in the solution phase [see eq. (S12)].

## B. Details of the Finite Element Approximation

On the right-hand side (r.h.s.) of eqs. (S11), (S12) and (S15), the integrals over cell  $N$  are calculated by summing the elemental contributions obtained by integration over the triangular elements adjoining node  $N$  (see Figs. S1a and S1b). Within an individual element, the linear approximation of function  $g$  given by the nodal values  $g_n$ ,  $n = 1, 2, 3$ , is provided by

$$g(\mathbf{x}) = \sum_{n=1}^3 g_n l_n(\mathbf{x}) , \quad (\text{S25})$$

where  $l_n(\mathbf{x})$  are the linear triangular shape functions shown in Fig S3. Hereafter, we omit the element labels and the global node labels when it does not lead to an ambiguity.

Note that the hat-function  $\Phi_N(\mathbf{x})$  is the union of the shape functions  $l_1(\mathbf{x})$  defined in the elements constituting cell  $N$  (see Figs. S1a and S1c). Hence, the integral  $\int \Phi_N(\mathbf{x}) g(\mathbf{x}) d\mathbf{x}$  is

decomposed to the elemental contributions of the form  $\sum_{n=1}^3 g_n \int l_1(\mathbf{x}) l_n(\mathbf{x}) d\mathbf{x}$ . The integration of the products of the functions  $l_n(\mathbf{x})$ ,  $n = 1, 2, 3$ , is known to yield the following result [1]:

$$\int l_1^a(\mathbf{x}) l_2^b(\mathbf{x}) l_3^c(\mathbf{x}) d\mathbf{x} = 2A \frac{a!b!c!}{(a+b+c+2)!} \quad , \quad (\text{S26})$$

where  $A$  is the area of the triangle. Thus, the elemental contributions to the r.h.s. of eq. (S11) and to the last term on the r.h.s. of eq. (S12) are calculated as

$$\int l_1(\mathbf{x}) g(\mathbf{x}) d\mathbf{x} = \frac{A}{12} (2g_1 + g_2 + g_3) \quad , \quad (\text{S27})$$

where the  $g_n$  correspond to the nodal values of the rate functions  $G$  or  $F$ .

To determine the elemental contribution to the second term on the r.h.s. of eq. (S12), it should be taken into account that

$$\nabla l_n(\mathbf{x}) = \frac{\mathbf{e}_3 \times \mathbf{d}_n}{2A} \quad , \quad (\text{S28})$$

where  $\mathbf{d}_n$ ,  $n = 1, 2, 3$ , are the edge vectors defined as shown in Fig. S2, and that the volume fraction of polymer in the element is constant and equal to

$$\phi = \phi_0 \frac{A_0}{\lambda_{\perp} A} \quad (\text{S29})$$

Here,  $\phi_0$  and  $A_0$  are the volume fraction of polymer and area of an element in the undeformed state, respectively. In eq. (S13), the concentration of the activator in solution  $\mathbf{u}$  and velocity of polymer  $\mathbf{v}_p$  are approximated using eq. (S25) through the respective nodal values  $\mathbf{u}_n$  and  $\mathbf{v}_n$ ,  $n = 1, 2, 3$ . Application of eqs. (S26), (S28), and (S29) results in the following equation for the elemental contribution to the second term on the r.h.s. of eq. (S12):

$$\int (\mathbf{J}_u \cdot \nabla l_1) d\mathbf{x} = \mathbf{d}_1 \cdot \mathbf{J}_{el} \quad (\text{S30})$$

In the above equation, the elemental flux  $\mathbf{J}_{el}$  is defined as

$$\mathbf{J}_{el} = \frac{1}{24} \sum_{n,m=1}^3 \mathbf{u}_n (1 + \delta_{nm}) (\mathbf{e}_3 \times \mathbf{v}_m) - \frac{1-\phi}{4A} \sum_{n=1}^3 \mathbf{u}_n \mathbf{d}_n \quad , \quad (\text{S31})$$

where  $\delta_{nm}$  is Kronecker's delta.

Equations (S17) and (S18) were obtained from eq. (S15) by using the following equation for the elemental contribution:

$$\phi_0 \phi^{-1} M(\phi) \int l_1(\nabla \cdot \hat{\boldsymbol{\sigma}}) d\mathbf{x} = AM(\phi) [-c_0 (\nabla l_1 \cdot \hat{\mathbf{B}}) + \phi_0 \phi^{-1} P(\phi, v) \nabla l_1] \quad , \quad (\text{S32})$$

The stress tensor  $\hat{\boldsymbol{\sigma}}$  was calculated according to eqs. (11) and (12). The second term in the parentheses on the r.h.s. of the above equation is equivalent to the second term on the r.h.s. of eq. (S18) owing to eqs. (S28) and (S29).

It is important to note that the Finger strain tensor  $\hat{\mathbf{B}}$  is constant within each element (but is different in different elements, of course) because the deformation of gel  $\mathbf{X} \rightarrow \mathbf{x}(\mathbf{X})$  is described by linear functions of the nodal coordinates. Specifically, as noted above in the Section A [see the discussion after eq. (S5)],  $\Phi_N(\mathbf{x}, t) = \Phi_N(\mathbf{X}, 0)$ , which means that the deformation is described as

$$\mathbf{x}(\mathbf{X}) = \sum_{n=1}^3 L_n(\mathbf{X}) \mathbf{x}_n \quad , \quad (\text{S33})$$

where  $L_n(\mathbf{X})$ ,  $n = 1, 2, 3$ , are the shape functions similar to those displayed in Fig. S3 but defined in the undeformed state. The Finger strain tensor is defined as  $\hat{\mathbf{B}} = \hat{\mathbf{F}} \cdot \hat{\mathbf{F}}^T$ , where  $\hat{\mathbf{F}} = \nabla_0 \mathbf{x}(\mathbf{X})$  is the deformation-gradient tensor [6,7]; the subscript “0” denotes differentiation with respect to coordinates in the undeformed state, i.e.,  $\mathbf{X}$ . The tensor  $\hat{\mathbf{F}}$  can be readily calculated by applying the operator  $\nabla_0$  to eq. (S33) and taking into account eq. (S28) re-written in the form  $\nabla_0 L_n(\mathbf{X}) = (2A_0)^{-1} (\mathbf{e}_3 \times \mathbf{D}_n)$ . Here,  $\mathbf{D}_n$ ,  $n = 1, 2, 3$ , are the edge vectors in the undeformed state (see Fig. S2). Hence, the following equation for the strain tensor was obtained:

$$\hat{\mathbf{B}} = (2A_0)^{-2} \sum_{n,m=1}^3 (\mathbf{D}_n \cdot \mathbf{D}_m) \mathbf{x}_n \mathbf{x}_m \quad , \quad (\text{S34})$$

where  $\mathbf{x}_n \mathbf{x}_m$  is a dyadic tensor. Finally, the result of dot-product of  $\nabla l_1$  according to eq. (S28) and the above strain tensor can be written in the following form:

$$\nabla l_1 \cdot \hat{\mathbf{B}} = (2A_0)^{-2} [-(\mathbf{D}_1 \cdot \mathbf{D}_3) \mathbf{d}_2 + (\mathbf{D}_1 \cdot \mathbf{D}_2) \mathbf{d}_3] \quad (\text{S35})$$

Substitution of eq. (S35) into eq. (S32) leads to eq. (S18).

### References

1. O. C. Zienkiewicz and R. L. Taylor, *The Finite Element Method*, Butterworth-Heinemann, Oxford, England, 2000.
2. P. Espanol and I. Zuniga, *J. Chem. Phys.*, 2009, **131**, 164106.1-164106.13.

3. P. Espanol, J. G. Anero and I. Zuniga, *J. Chem. Phys.*, 2009, **131**, 244117.1-244117.15.
4. V. V. Yashin and A. C. Balazs, *J. Chem. Phys.*, 2007, **126**, 124707.1-124707.17.
5. V. V. Yashin and A. C. Balazs, *Phys. Rev. E: Stat., Nonlinear, Soft Matter Phys.*, 2008, **77**, 046210.1-046210.7.
6. J. Bonet and R. D. Wood, *Nonlinear Continuum Mechanics for Finite Element Analysis*, Cambridge University Press, New York, 1997.
7. A. D. Drozdov, *Finite Elasticity and Viscoelasticity: A Course in the Nonlinear Mechanics of Solids*, World Scientific, Singapore, 1996.

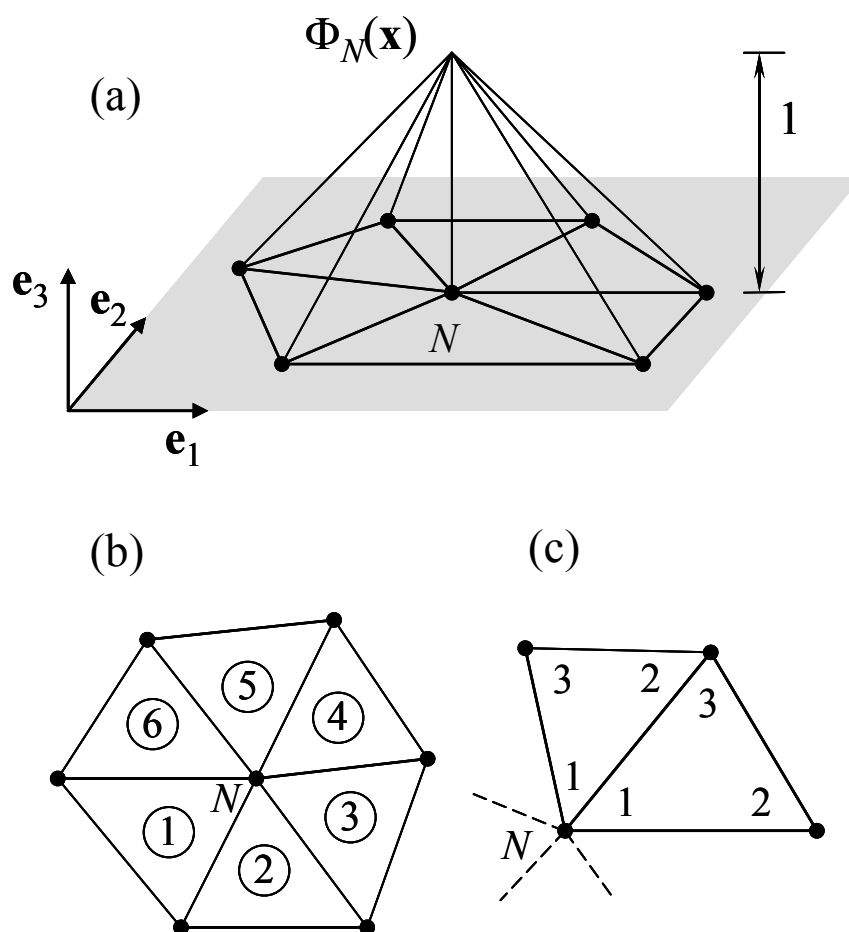


**Fig. S1**

The cell  $N$  in a triangular mesh. (a) The hat-function  $\Phi_N(\mathbf{x})$ . (b) Labeling of the elements within the cell. (c) Labeling of the nodes within the elements.

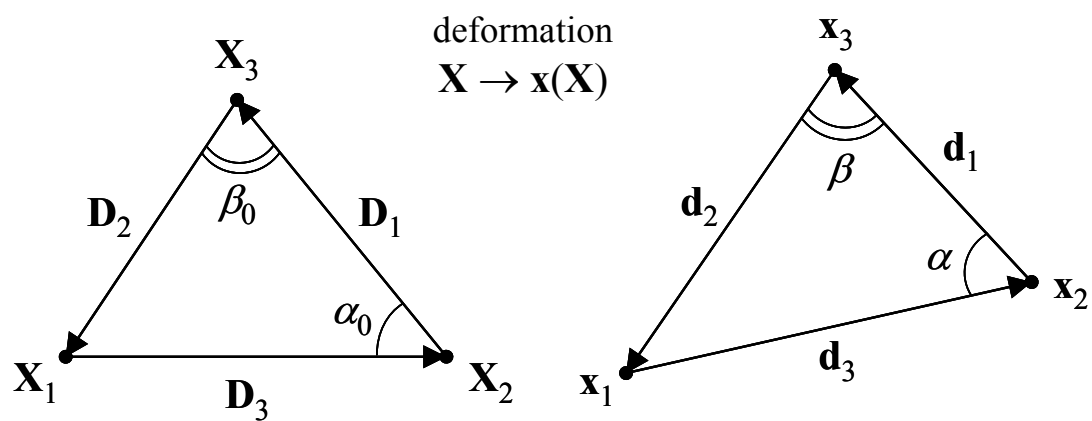


**Fig. S2**

A triangular element before (left) and after (right) deformation  $\mathbf{X} \rightarrow \mathbf{x}(\mathbf{X})$ .

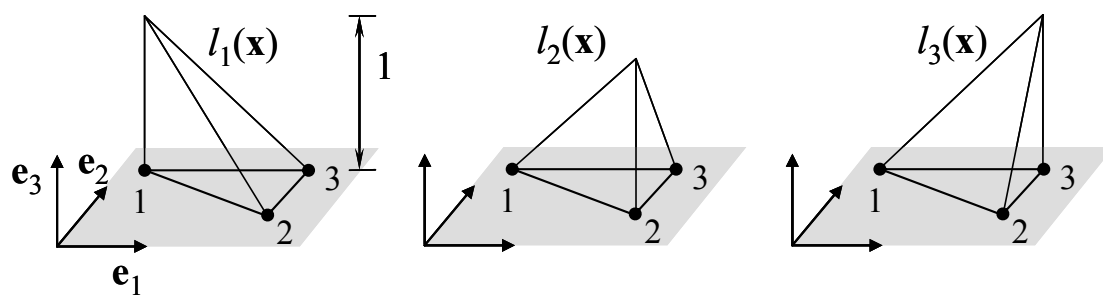


**Fig. S3**

The linear triangular shape functions  $l_n(\mathbf{x})$ ,  $n = 1, 2, 3$ , used in the finite element approximation.